Zooanthroponotic transmission of SARS-CoV-2 and host-specific viral mutations revealed by genome-wide phylogenetic analysis

Sana Naderi[1], Peter E. Chen[1,2], Carmen Lía Murall[1,3], Raphael Poujol[4], Susanne Kraemer[3], Bradley S. Pickering[5,6,7], Selena M. Sagan[1,8*], B. Jesse Shapiro[1,9*]

1. Department of Microbiology & Immunology, McGill University, Montreal, QC, Canada
2. Département de sciences biologiques, Université de Montréal, Montreal, QC, Canada
3. Public Health Agency of Canada, Winnipeg, MB, Canada
4. Research Centre, Montreal Heart Institute, Montreal, QC, Canada
5. National Centre for Foreign Animal Disease, Canadian Food Inspection Agency, Winnipeg, MB, Canada
6. Department of Veterinary Microbiology and Preventative Medicine, College of Veterinary Medicine, Iowa State University, Ames, Iowa, USA
7. Department of Medical Microbiology and Infectious Diseases, University of Manitoba, Winnipeg
8. Department of Biochemistry, McGill University, Montreal, QC, Canada
9. McGill Genome Centre, Montreal, QC, Canada

*for correspondence: selena.sagan@mcgill.ca; jesse.shapiro@mcgill.ca

Abstract

Severe Acute Respiratory Syndrome Coronavirus 2 (SARS-CoV-2) is a generalist virus, infecting and evolving in numerous mammals, including captive and companion animals, free-ranging wildlife, and humans. Transmission among non-human species poses a risk for the establishment of SARS-CoV-2 reservoirs, makes eradication difficult, and provides the virus with opportunities for new evolutionary trajectories, including selection of adaptive mutations and emergence of new variant lineages. Here we use publicly available viral genome sequences and phylogenetic analysis to systematically investigate transmission of SARS-CoV-2 between human and non-human species and to identify mutations associated with each species. We found the highest frequency of animal-to-human transmission from mink, compared with negligible transmission from other sampled species (cat, dog, and deer). Although inferred transmission events could be limited by sampling biases, our results provide a useful baseline for further studies. Using genome-wide association studies, no single nucleotide variants (SNVs) were significantly associated with cats and dogs, potentially due to small sample sizes. However, we identified three SNVs statistically associated with mink and 26 with deer. Of these SNVs, ~⅔ were plausibly introduced into these animal species from local human populations, while the remaining ~⅓ were more likely derived in animal populations and are thus top candidates for experimental studies of species-specific adaptation. Together, our results highlight the importance of studying animal-associated SARS-CoV-2 mutations to assess their potential impact on human and animal health.

Importance. SARS-CoV-2, the causative agent of COVID-19, can infect many animal species, making eradication difficult because it can be reseeded from different reservoirs. When viruses replicate in different species, they may be faced with different evolutionary pressures and acquire new mutations, with unknown consequences for transmission and virulence in humans. Here we analyzed SARS-CoV-2 genome sequences from cats, dogs, deer, and mink to estimate transmission between each of these species and humans. We found several transmission events from humans to each animal, but very few detectable transmissions from animals back to humans, with the exception of mink. We also identified three mutations more likely to be found in mink than humans, and 26 in deer. These mutations could help the virus adapt to life in these different species. Ongoing surveillance of SARS-CoV-2 from animals will be important to understand their potential impacts on both human and animal health.

Introduction

Coronaviruses can have broad animal host ranges, and severe acute respiratory syndrome coronavirus-2 (SARS-CoV-2) is no exception. Although the animal reservoir of ancestral SARS-CoV-2 remains unknown, SARS-CoV-2 has close relatives in bats and an ancestral variant likely spilled over into humans via an intermediate animal host in a seafood market in Wuhan, China (Worobey et al. 2022). Although SARS-CoV-2-related coronaviruses from animals in the Wuhan market were not sampled, there have been several subsequent reports of SARS-CoV-2 transmission ("spillback") from humans to animals including in farmed mink (Oude Munnink et al. 2021) and wild white-tailed deer (*Odocoileus virginianus*) (Kuchipudi et al. 2022; Kotwa et al. 2022). Consequently, transmission among potential animal reservoirs is a key feature of the past and future evolution of coronaviruses. In addition to making SARS-CoV-2 elimination highly unlikely, evolution in animal reservoirs could transiently increase evolutionary rates (Porter et al. 2022) and potentially select for novel mutations with effects on transmission and virulence in humans (Otto et al. 2021). Viral adaptation to one host species might result in the tradeoff of reduced transmission in other species. Alternatively, it could permit significant genetic drift, opening up new peaks in the human-adaptive fitness landscape. For example, it is speculated that the SARS-CoV-2 Omicron variant of concern (VOC) might have evolved in a non-human animal (possibly rodent) before transmitting widely among humans (Wei et al. 2021). Although this scenario remains hypothetical and is not exclusive of other hypotheses involving evolution in unsampled human populations or a chronically infected individual, it illustrates the potential dramatic consequences of evolution in animal reservoirs. Ongoing transmission among humans and non-human animals and its implications for viral evolution and host adaptation thus deserves further study.

There have been several reports of SARS-CoV-2 transmission from humans to individual species of animals, and in some cases back to humans. In addition to farmed mink (Oude Munnink et al. 2021), there have also been reports of transmission from pet hamsters (Yen et al. 2022) and possible transmission events from white-tailed deer to humans in North America (Pickering et al. 2022). Evidence suggests that certain mutations may improve replication fitness of SARS-CoV-2 in animal hosts. For instance, experimental infections of mink (*Neovison vison*) and ferret *(Mustela furo*) identified mutations within the viral spike (S) protein that increase binding to the ACE2 receptor in these animals, while decreasing infection of human airway cells (Zhou et al. 2022). One of these mutations (S:N501T) was also found to be prevalent in infected mink sampled in the United States (Cai and Cai 2021; Eckstrand et al. 2021).

While such case studies have been valuable in highlighting patterns of transmission and adaptation across individual animal species since the beginning of the pandemic, a standardized, global analysis of the available data is lacking. In this study, we comprehensively compared SARS-CoV-2 sequences derived from animal hosts using a broad dataset. Using phylogenetic methods, we inferred transmission events between humans and four other frequently infected animals and quantified their relative frequencies. Our analysis revealed a relatively high number of mink-to-human transmission events, while instances of animal-to-human transmission from cats (*Felis catus domesticus)*, dogs (*Canis lupus familaris),* or deer (*Odocoileus virginianus*) were rare. Using genome-wide association studies (GWAS), we also identified mutations associated with specific animal species. We recovered the S:N501T mutation previously associated with mink, along with two other amino acid changes in other SARS-CoV-2 genes. We also identified several novel mutations associated with deer, including both synonymous and nonsynonymous substitutions. Together, our work provides a quantitative framework for tracking SARS-CoV-2 transmission across animals from available genomic sequences and points to several candidate animal-adaptive mutations for experimental follow-up.

Results

Although secondary spillover events of SARS-CoV-2 transmission from animals back to humans have been reported, their frequency has yet to be quantified and compared across animal species. To this end, we retrieved all available SARS-CoV-2 genome sequences sampled from non-human animals from GISAID (**Supplementary Table S1**). After applying sequence quality filters (**Supplementary Table S2**) and considering only animals with 30 or more sequences, we were left with four species: cat, dog, mink and deer. Our filters excluded common experimental animals such as mice and ferrets. For each of the four animal species, we extracted a similar number of closely-related human-derived sequences (Methods). If these closely-related animal-human pairs represent recent transmission chains, we would expect them to come from the same geographic region. Consistent with this expectation, we found that 95.4% of deer-derived sequences share the same sampling location as their close human-derived relatives, and this percentage is slightly lower for cat (85.6%), dog (89%), and mink (91.7%). The high percentage for deer could be due to higher sampling effort in North America, the origin of all deer sequences. More generally, the variation in these percentages could be explained by other sampling biases. For example, cats and dogs might be undersampled relative to mink and deer.

To investigate potential animal-to-human transmission events in greater detail, including the direction of transmission, we used ancestral state reconstruction on viral phylogenetic trees. We are aware that such ancestral state reconstruction can be biased by differential sampling across species. Our goal is, therefore, not to infer absolute rates of cross-species transmission, but rather to provide a consistent comparative framework for interspecies transmission. For each candidate species, the animal-derived sequences, and their closest relative human-derived sequence were combined with ten random sub-samplings of human-derived sequences (n ≈ 50 per subtree per month of the pandemic), from which we inferred ten replicate phylogenies per species, providing an assessment of phylogenetic uncertainty. Using ancestral state reconstruction as previously described (Murall et al. 2021), we counted the most basal animal-to-human (**Figure 1a-d**) and human-to-animal transitions on each tree (**Supplementary Table S3**). Representative detailed trees are available in **Supplementary Figures S1-S4.** To determine a lower bound for the transmission counts, we excluded transition branches with <75% bootstrap support (Methods). As further validation, we performed a permutation test to determine whether the estimated transmission counts converged on a non-random value. We performed the same ancestral state reconstruction on 1000 permutations of each of the 40 phylogenies whose tip labels (animal or human) were shuffled randomly, and the number of transmissions in both directions were recorded. This permutation test revealed that in both directions (animal-to-human and human-to-animal) the observed transmission counts in mink, deer, and cat falls within a narrow range (standard deviations of 27.74, 1.29, and 0.52 respectively) compared to the permutations (266.06, 2.84, and 1.87) while the observed counts in dog (standard deviation of 1.10) is similar to the permutations (0.91). In the human-to-animal direction, the observed standard deviations in transmission counts are 0.48, 0.73, 2.17, and 2.17 for cat, dog, mink and deer, respectively, compared to permuted values of 6.66, 1.70, 186.05, and 16.46. These results show that, in general, our inference of transmission events converges on a non-random value but that the estimate for dog-to-human transmission might be less reliable.

Based on the bootstrap-filtered counts, we inferred less than one transmission event from animals back to humans on average from cats, dogs, and deer (**Figure 1e, Table 1**). In contrast, there were an average of 12 or more transmission events inferred from mink to human. The upper bound (bootstrap unfiltered) estimates are higher, but the pattern of much higher transmission from mink is retained. The inferred number of transmissions in the opposite direction, from human-to-animal, was generally higher and much more uniform across species (**Figure 1f, Table 1**), with

lower bounds in the range of 4.6 to 12.8 events. However, the higher sampling of human-derived compared with animal-derived sequences may have inflated the human-to-animal events relative to the animal-to-human events. Mink are also better sampled than the other animal species (**Table 1**), and further sampling of other animals could identify more transmission events. Despite these caveats, it is notable that human-to-animal transmission events are relatively constant across animal species, while mink-to-human transmission is much higher (or at least more frequently detected) compared with other animals.

Table 1: Average inferred transmission events between humans and animals.

Average inferred number of transitions (filtered – unfiltered)	Mink (n=1038)	Deer (n=134)	Cat (n=78)	Dog (n=39)
Animal-to-human	12.5 – 108.3	0.3 – 1.1	0 – 4.4	0.1 – 1.6
Human-to-animal	12.8 – 65.4	11.6 – 59.5	8.5 – 68.3	4.6 – 35.0

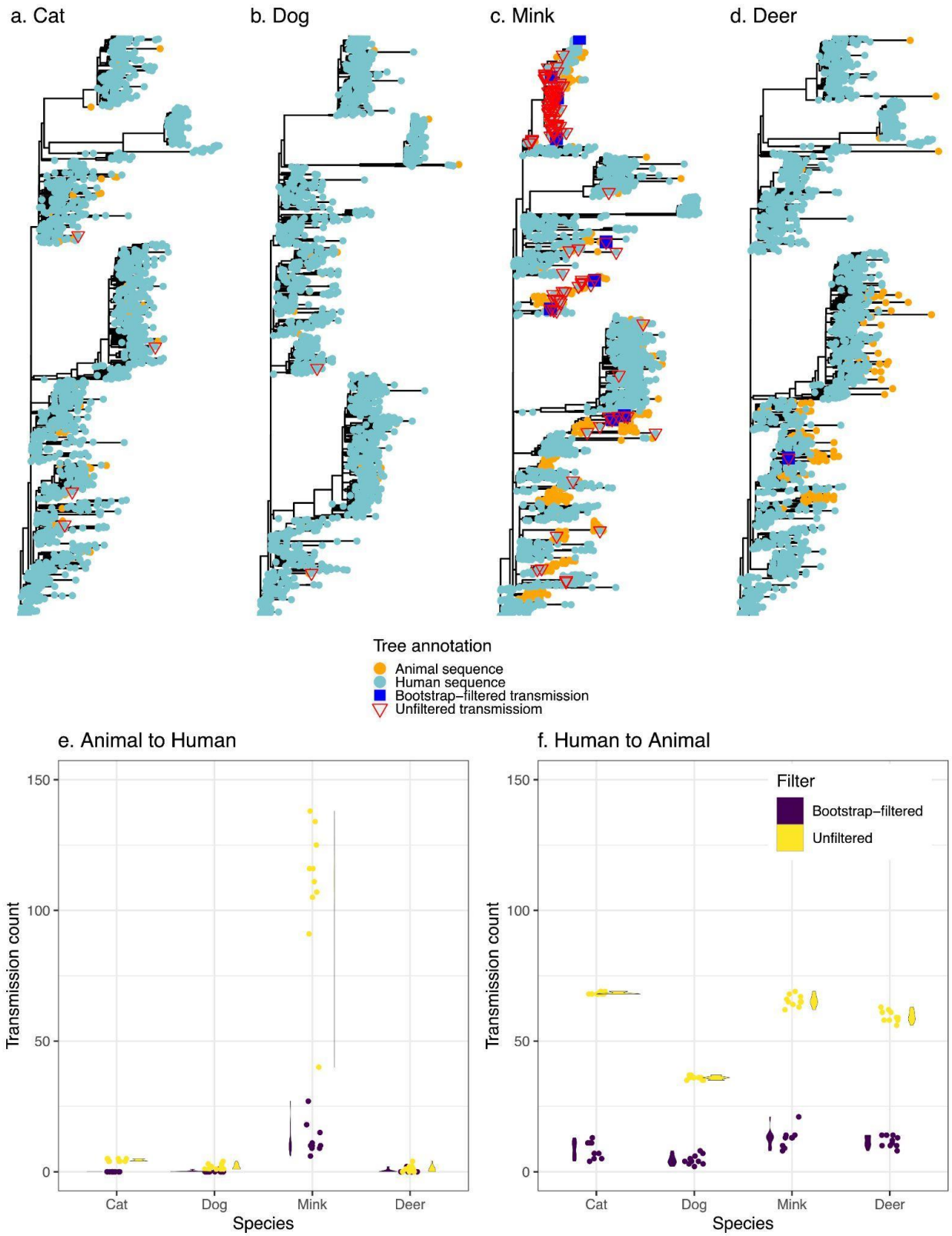

Figure 1. Transmission events inferred between humans and animals. Panels a-d display a representative tree for every species with animal to human transmissions marked on the tree. More detailed versions of these trees are in **Supplementary Figures S1-S4**. Trees are rooted with the Wuhan reference

genome. Panels e and f display the distribution (violin plots alongside points plotted with jitter to avoid overlap) of inferred transmission counts (across 10 replicate trees) in each animal species, in both bootstrap-filtered and unfiltered trees.

Next, we sought to identify mutations associated with particular animal species compared to humans. These mutations could be candidates for species-specific adaptations. To do so, we conducted GWAS using POUTINE, a method which implicitly controls for population structure and linkage (non-independence) between mutations by considering only homoplasic mutations that are identical by state, but not identical by descent, and that have occurred independently multiple times in the phylogeny (Chen and Shapiro 2021). We performed a separate GWAS to identify mutations associated with each species, and replicated the GWAS on each of the ten replicate trees described above.

We identified numerous single nucleotide variants (SNVs) with high statistical significance associated with mink and deer, but none in cats or dogs (**Figure 2**). In all cases, we used a significance cutoff of a family-wise $p < 0.05$ to correct for multiple hypothesis testing. The mink GWAS revealed three unique SNVs (**Table 2**). One of these hits appears in all ten replicates and the remaining two appear in at least half of the replicates. All three of these mutations are non-synonymous, including S:N501T which was previously associated with a mink outbreak in the United States (Cai and Cai 2021). Inspecting the distributions of these GWAS hits across the tree reveals several independent origins (**Figure S3**). For example, S:N501T occurred independently in The Netherlands, Denmark, Latvia, Lithuania, Spain, France, and the USA (**Figure S3**), explaining the strong association detected by POUTINE. The deer GWAS revealed a total of 26 unique statistically significant SNVs, of which seven appear in all ten replicates, and five in at least half the runs (**Table 3**). Out of these 26 hits, five are intergenic (within the 5′ and 3′ UTRs) and 12 are synonymous mutations. Notably, 21 of the hits are C>U transition mutations. The seven hits found in all ten replicates clearly occur multiple times independently in different branches of the tree; for example, ORF1ab:N4899I (which affects amino acid 507 of the mature RNA-dependent RNA polymerase protein, nsp12) occurs at least twice independently in both the states of New York and Iowa (**Figure S4**).

We next asked whether mutations identified by GWAS plausibly occurred in an animal host or if they were more likely circulating in a local human population before being transmitted to a different animal host. While both these categories of mutations are statistically associated with a particular

animal species, the former are particularly good candidates for animal-specific adaptations. To address this question, we obtained the global frequency of the minor allele of each significant GWAS hit in Cov-Spectrum (C. Chen et al. 2021) – a significantly larger database than our downsampled trees used for GWAS. The minor alleles were generally rare (<1% frequency; **Supplementary Tables S4 & S5**), as expected for animal-associated mutations in a large database dominated by human sequences. To test the hypothesis that animal-associated mutations arose not in animals but in a local human population that then transmitted to animals in the same region, for each GWAS hit we first defined the "in" region in which the animals containing the mutation were sampled and the "out" regions including all other regions. We then performed a Fisher's exact test to determine if human-derived sequences containing the animal-associated mutation were enriched in the "in" region, resulting in an odds ratio (OR) significantly higher than 1 (Methods). For mink, two GWAS hits had OR significantly greater than 1 ($P < 0.0001$, **Table 2**). Only the S:N501T mutation had OR significantly less than 1, making it the best candidate for having arisen in a mink host, rather than in a human who later transmitted the mutant virus to a mink. For deer, the majority of GWAS hits (18/26) could be explained by transmission from the local human population (OR > 1) while the remaining eight could not (OR < 1 or not significantly different than 1, **Table 3**).

Table 2. **Single-nucleotide variants associated with mink by GWAS.** "Pos" refers to the nucleotide position in the reference genome. Homoplasy counts in focal animals (cases), humans (controls), and *P*-values are averaged across replicates in which the site's family-wise *P*-values was < 0.05. Where applicable, amino acid positions refer to the polyprotein with mature protein positions in parenthesis. The 'local transmission odds ratio' is the result of a Fisher's exact test of the likelihood that the alternate base (animal-associated minor allele) was enriched in the local human population where the mink sequences bearing the alternate base were sampled (Methods). n.s., not significant. Odds ratio *P*-values: * < 0.05, ** < 0.01, *** < 0.001.

Pos.	Ref. base	Alt. base	Amino acid change	Gene	Homoplasy count in focal animal	Homoplasy count in humans	*P*-value (pointwise)	*P*-value (familywise)	Significant in N replicates	Local transmission odds ratio
26047	U	G	L219V	ORF3a	6	0	0.0014	0.0365	10	3.93***
12795	G	A	G4177E (nsp9 G37E)	ORF1ab/pp1ab/nsp9/replicase	6	0	0.0015	0.0368	6	7.53***
23064	A	C	N501T	Spike/S1/RBD/binds ACE2	6.4	0	0.0010	0.0258	5	0.48***

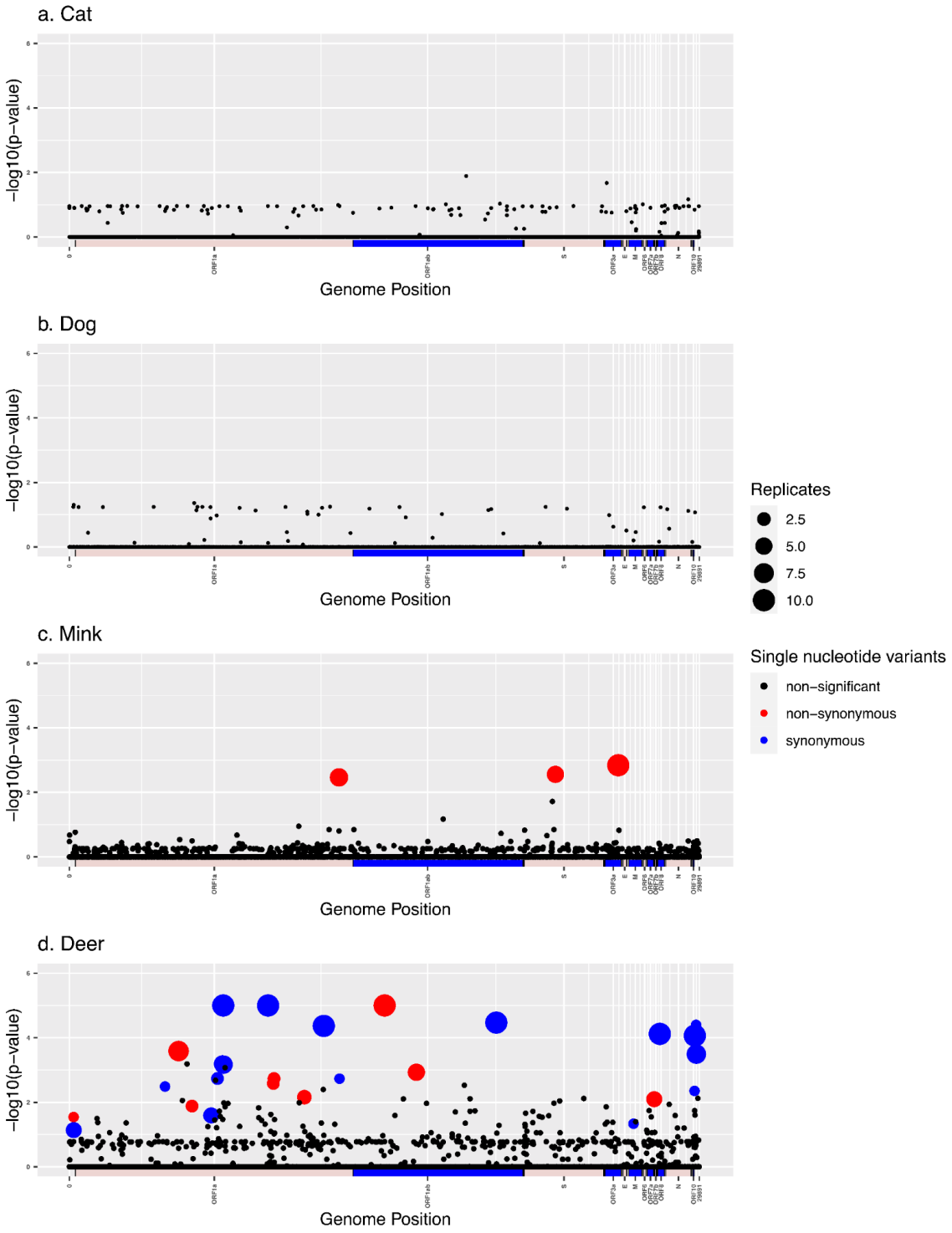

Figure 2: Manhattan plots summarizing GWAS hits in each animal species. In every panel, the x-axis represents the nucleotide position in the SARS-CoV-2 reference genome and the y-axis represents the -log10 of the pointwise *p*-values averaged over replicates. ORFs are shown as alternating blue and pink horizontal bars along the x-axis. Statistically significant hits with family-wise corrected *p*-values of lower

than 0.05 are shown in red (non-synonymous) or blue (synonymous), while non-statistically significant p-values are in black.

Table 3. **Single-nucleotide variants associated with deer by GWAS**. "Pos" refers to the nucleotide position in the reference genome. Homoplasy counts in focal animals (cases), humans (controls), and *P*-values are averaged across replicates in which the site's family-wise *P*-values was < 0.05. Where applicable, amino acid positions refer to the polyprotein with mature protein positions in parenthesis. IG, Intergenic. The 'local transmission odds ratio' is the result of a Fisher's exact test of the likelihood that the alternate base (animal-associated minor allele) was enriched in the local human population where the deer sequences bearing the alternate base were sampled (Methods). n.s., not significant. Odds ratio *P*-values: * < 0.05, ** < 0.01, *** < 0.001.

Pos.	Ref. base	Alt. base	Amino acid change	Gene	Homoplasy count in focal animal	Homoplasy count in humans	*P*-value (pointwise)	*P*-value (familywise)	Significant in N replicates	Local transmission odds ratio
7303	C	U	I2346I (nsp3 1524)	ORF1a/pp1ab /pp1a/nsp3	17.8	1.2	9.99E-06	9.99E-06	10	2.51***
9430	C	U	I3055I (nsp4 I292I)	ORF1a/pp1ab /pp1a/nsp4	15.2	6.2	9.99E-06	9.99E-06	10	2.20***
14960	A	U	N4899I (nsp12 N507I)	ORF1ab/pp1ab/nsp12/RdRp	7.8	0.1	9.99E-06	1.09E-05	10	0**
20259	C	U	F6665F (nsp15 F213F)	ORF1ab/pp1ab/nsp15	4.8	0.1	3.39E-05	0.0013	10	n.s.
28016	C	U	F41F	ORF8	4	0	7.59E-05	0.0061	10	6.09***
12073	C	U	D3936D (nsp7 D67D)	ORF1a/pp1ab /pp1a/nsp7	5.2	1.1	4.29E-05	0.0025	10	n.s.
29679	C	U	IG	3'UTR	5	1.8	8.59E-05	0.0055	10	3.17***
5184	C	U	P1640L (nsp3 P822L)	ORF1a/pp1ab /pp1a/nsp3	4.6	1.6	0.0002	0.0115	8	2.61***
29750	C	U	IG	3'UTR/S2M	5	2.6	0.0002	0.0103	7	3.12***
7318	C	U	F2351F (nsp3 F1533F)	ORF1a/pp1ab /pp1a/nsp3	4	0.3	0.0001	0.0114	6	3.80***
16466	C	U	P5401L (nsp13 P77L)	ORF1ab/pp1ab/nsp13/Hel	5	1	4.99E-05	0.0019	5	4.09***
7267	C	U	F2334F (nsp3 F1516F)	ORF1a/pp1ab /pp1a/nsp3	4.4	0.8	9.39E-05	0.0079	5	2.79***
210	G	U	IG	5'UTR/SL5a	4	0.5	0.0001	0.0136	4	3.98***
6730	C	U	N2155N (nsp3 N1337N)	ORF1a/pp1ab /pp1a/nsp3	4	0.75	0.0002	0.0168	4	1.81**
27752	C	U	T120I	ORF7a	4	0.75	0.0002	0.0169	4	4.03***

11152	C	U	V3629V (nsp6 V60V)	ORF1a/pp1ab /pp1a/nsp6	4	0.7	0.0002	0.0153	3	0.80**
5822	C	U	L1853F (nsp3 L1035F)	ORF1a/pp1ab /pp1a/nsp3	4	0.5	0.0001	0.0118	2	n.s.
9711	C	U	S3149F (nsp4 S386F)	ORF1a/pp1ab /pp1a/nsp4	4	0.5	8.49E-05	0.0118	2	0.56**
9679	C	U	F3138F (nsp4 F375F)	ORF1a/pp1ab /pp1a/nsp4	4	0	9.49E-05	0.0067	2	2.32***
7029	C	U	S2255F (nsp3 S1437F)	ORF1a/pp1ab /pp1a/nsp3	4	0.5	0.0002	0.0149	2	0.22***
29738	C	A	IG	3'UTR/S2M	4	0	3.99E-05	0.0059	1	n.s.
26767	U	C	I82T	ORF5/M	4	0	8.99E-05	0.0057	1	4.09***
203	C	U	IG	5'UTR/SL5a	4	1	0.0003	0.0191	1	5.94***
12820	A	G	L4185L (nsp9 L45L)	ORF1a/pp1ab /pp1a/nsp9	5	1	3.99E-05	0.0009	1	4.52***
4540	C	U	Y1425Y (nsp3 Y607Y)	ORF1a/pp1ab /pp1a/nsp3	4	1	0.0002	0.0239	1	2.80***
29666	C	U	L37F	ORF10	4	1	0.0002	0.0219	1	1.54***

Discussion

SARS-CoV-2 transmission between humans and animals has typically been studied in individual species in isolation, and using heterogeneous methods and datasets. Similarly, viral mutations associated with particular species have been reported, but largely in experimental studies or region-specific sampling efforts that are difficult to generalize. Our goal in this study was to apply standardized methods to identify animal-to-human transmission events and to discover animal-associated mutations using viral genomic data readily available to date. The results are necessarily biased by sampling effort. Specifically, oversampling of human-derived sequences could bias the ancestral state reconstruction toward human-to-animal rather than animal-to-human transmission. In the future, such biases could be avoided using a Bayesian structured coalescent approximation (De Maio et al. 2015). Our approach nevertheless provides a 'level playing field' upon which to assess the results of previous animal-specific studies. Our study also provides a pipeline for researchers to assess the transmission and evolution of SARS-CoV-2 within animals and between animals and humans.

Consistent with previous reports (Oude Munnink et al. 2021), mink had the largest number of inferred transmission events to humans. This could be because mink have more opportunities to interact with humans on mink farms, whereas contact between deer and humans is more limited and potentially seasonal (Kuchipudi et al. 2022). However, mink outbreaks could be more frequently reported due to higher surveillance of mink farms and noticeable symptomatic disease in these animals (Oreshkova et al. 2020). As for cats and dogs, we inferred much lower transmission to humans, suggesting that they might be “dead-ends” for the virus. This does not mean that SARS-CoV-2 transmission from dogs or cats to humans is not possible, and it may be more readily detected with deeper sampling or in prospective household transmission studies. Nonetheless, transmission from humans to animals was remarkably uniform across species and small differences across species may be explained by sampling effort. Overall, our results support the previous reports of relatively high rates of mink to human transmission, and only rare or anecdotal transmission from other animals, such as deer (Pickering et al. 2022).

Despite the large sample size of mink-derived viral sequences, we only detected three mink-associated SNVs using GWAS, including the previously identified S:N501T mutation. This is consistent with relatively little time for SARS-CoV-2 to adapt to mink between transmission cycles in humans. In contrast, we detected many more SNVs associated with deer despite a smaller sample size. Even if we only consider the eight SNVs less likely to have arisen in human population before transmitting to deer, or the seven SNVs detected in all replicate GWAS runs, there are still more than twice as many deer-associated than mink-associated GWAS hits. This could suggest a greater number of deer-adapted SNVs compared to mink-adapted SNVs, perhaps due to multiple uninterrupted cycles of deer-deer transmission. Sustained deer-deer transmission is also supported by previous studies (Kuchipudi et al. 2022), including the observation of relatively divergent SARS-CoV-2 genomes (Pickering et al. 2022). Asymptomatic or mild disease in deer relative to mink (Oreshkova et al. 2020) might also allow more opportunity for evolution and transmission during prolonged infections. Despite pruning out highly divergent branches, including several of the Canadian sequences involved in a potential deer-to-human transmission event (Pickering et al. 2022), some relatively long deer-associated branches are notable in our study (**Figure 1d**). Together, these results point to deer as an important reservoir of novel SARS-CoV-2 mutations. Ongoing monitoring of deer-to-human transmission events is therefore warranted.

304 Several viral mutations have been previously associated with cat and dog (Elaswad et al. 2020),
305 but we found no statistically significant mutations associated with either of these species. This
306 could be due to limited viral adaptation, which would be expected if cats and dogs are effectively
307 dead-end hosts for the virus, with little time for cycles of intra-species transmission. Alternatively,
308 the limited sample size for these species could have limited GWAS power to identify adaptive
309 mutations. Given the higher viral load and shedding in cats compared to dogs (Bosco-Lauth et al.
310 2020; Shi et al. 2020), we expect greater adaptation and transmission in cats; however, further
311 data will be needed to test this expectation.
312
313 We identified three statistically significant mutations associated with mink. The substitution
314 ORF3a:L219V, which appears in all ten GWAS replicates, has been previously detected as a
315 substitution associated with mink, in the ORF3a accessory gene (Elaswad et al. 2020). However,
316 the previous detection was not statistically tested for significance. Similarly, the ORF1ab:G4177E
317 (nsp9:G37E) mutation has been identified previously in mink-derived sequences (Eckstrand et al.
318 2021). The S:N501T substitution has also been previously associated with mink (Lu et al. 2021;
319 Elaswad et al. 2020) and ferret (Zhou et al. 2022), and the same site, has also been reported to
320 be adaptive in mice, with an S:N501Y amino acid substitution. The mink-associated S:N501T
321 substitution has been associated with increased binding to human ACE2 (Starr et al. 2020). The
322 S:N501Y substitution has been detected in several human SARS-CoV-2 VOCs with higher
323 transmissibility, such as the Alpha variant (Y. Liu et al. 2021; Vöhringer et al. 2021). Certain other
324 mutations that have been previously associated with mink, including S:Y453F (Zhou et al. 2022;
325 Lu et al. 2021; Elaswad et al. 2020) and S:L260F (Adney et al. 2022) that were suggested to arise
326 as a result of rapid adaptation, do not appear to be statistically significant mutations based on our
327 GWAS. While such mutations could be truly animal-associated and were not picked up in GWAS
328 due to limited power or sampling, others may be anecdotal reports that do not survive the scrutiny
329 of rigorous statistical testing, or associations identified in laboratory conditions that are not
330 currently observed in nature.
331
332 Many of the deer-associated mutations are synonymous and occur broadly across the genome
333 outside of the relatively well-studied spike (S) protein (**Figure 2**). These are primarily transition
334 mutations, which are typically generated at a higher frequency than transversions. The deer-
335 associated synonymous mutations showed no particular bias toward codons that are preferred in
336 deer relative to humans; therefore selection for codon usage optimization does not easily explain
337 these associations (data not shown). Nonetheless, the vast majority of mutations were C>U

338 transitions, which may be a reflection of APOBEC1-mediated RNA editing, which results in
339 deamination of cytosine to uracil in single-stranded RNA (Harris and Dudley 2015; Salter and
340 Smith 2018). Consistent with this hypothesis, C>U transitions in deer contained the consensus
341 sequence [U/A][U/A]C[A/U][A/U], which resembles that observed for human APOBEC1-mediated
342 deamination [AU]C[AU]; however, it remains to be seen whether the deer APOBEC1 isoform has
343 the same substrate specificity or whether there is increased APOBEC expression or activity in
344 deer tissue (Di Giorgio et al. 2020; Rosenberg et al. 2011)). Alternatively, the C>U transitions may
345 be related to RNA secondary structure or nucleotide composition biases required for genome
346 condensation during viral replication, organelle biogenesis, or virion assembly in the deer host.

347 Our GWAS revealed several mutations in deer that localized to distinct RNA secondary structures
348 in the 5´ and 3´ UTRs of the viral RNA. Specifically, in the 5´ UTR, both mutations (C203U and
349 G210U) localized to stem loop 5a (SL5a), a highly conserved stem-loop structure previously
350 implicated in virion assembly in related coronaviruses (Yang and Leibowitz 2015; Morales Lucia
351 et al. 2013; Miao et al. 2021). Similarly, in the 3´ UTR, all the mutations localized to the 3´ terminal
352 stem-loop structure, with two specifically localized to the S2M region (C29738A and C29750U)
353 (Yang and Leibowitz 2015; Gilbert and Tengs 2021; Wacker et al. 2020). Interestingly, while the
354 3´ terminal stem-loop structure is known to be hypervariable, the S2M region is highly conserved
355 in sequence and structure across a wide range of RNA viruses, including members of the
356 *Astroviridae*, *Caliciviridae*, *Picornaviridae,* and *Coronaviridae* families (Tengs et al. 2013; Gilbert
357 and Tengs 2021). While the role of this S2M region is poorly understood, its strict conservation
358 across a range of positive-strand RNA viruses suggests that it may play an important role in the
359 viral life cycle. Notably, both the mutations identified by GWAS are predicted to maintain the
360 overall S2M consensus fold, so these may reflect differences in species-specific interactions
361 between S2M and host proteins or RNA molecules.

362 The deer GWAS also revealed a few nonsynonymous mutations in viral proteins important in RNA
363 binding and host antiviral responses. Specifically, ORF1ab:N4899I (nsp12:N507I) lies in the
364 nsp12 RNA-dependent RNA polymerase, within the highly conserved motif G which is important
365 in positioning the 5´ template strand during viral RNA synthesis (Sheahan et al. 2020). While N507
366 is known to make contact with the +2 nucleotide of the template strand, experimental
367 investigations will be needed to understand how the N507I mutation impacts the active site
368 structure and/or viral RNA synthesis (Hillen et al. 2020). The ORF1ab:P5401L (nsp13:P77L)
369 mutation in the nsp13 helicase is predicted to be a solvent-exposed residue within the N-terminal
370 Zinc-binding domain (Newman et al. 2021). However, given that this is distant from the helicase

active site, we predict that it is unlikely to affect helicase enzymatic activity. Finally, we identified two mutations that may have implications for host adaptation as they are identified in proteins known to interact with the host antiviral response. Specifically, ORF1a:P1640L (nsp3:P822L) in the nsp3 protease localizes to the deubiquitinating site in the PLpro domain which overlaps with the ISG15 binding site, suggesting it may modulate host antiviral responses (Yang and Leibowitz 2015; Shin et al. 2020; G. Liu et al. 2021). Interestingly, the deer GWAS also revealed the ORF7a:T120I mutation within the ORF7a accessory protein. This residue is adjacent to K119, which is implicated in the inhibition of the antiviral response in human cells (Redondo et al. 2021; Cao et al. 2021). Specifically, K119 polyubiquitination has been shown to block STAT2 phosphorylation, leading to inhibition of type I IFN. Thus, it is possible that the ORF7a:T120I mutation modulates ubiquitination at the K119 residue; however, this will require experimental validation.

Upon finalization of this manuscript, another analysis of SARS-CoV-2 transmission and potential host adaptation was published, using a similar dataset from GISAID (Tan et al. 2022). Notably, this work focused only on transmission from humans to other animals, while we also considered the animal-to-human direction. The approach used to identify animal-associated mutations was conceptually similar to ours – focusing on homoplasic mutations and a set of reasonable but arbitrary filters for allele frequencies and effect sizes – whereas we took a more formal statistical GWAS approach. Our three mink GWAS hits are a subset of the four identified in the other study, and neither study identified any deer-associated mutations in Spike (Tan et al. 2022). Our study identified more significantly deer-associated mutations (including the single hit reported by Tan et al. in nsp3, ORF1a:L1853F (nsp3:L1035F), which could be due to different data filtering and significance testing approaches. Overall, the two studies are complementary, and pave the way for future studies on larger datasets.

In conclusion, while the dynamics of anthroponosis and zooanthroponosis for SARS-CoV-2 are still unclear, cross-species transmission events are likely to continue to occur given continued geographically widespread infections, high transmission rates, and the emergence of new variants. We identified several statistically significant animal-associated substitutions in mink and deer, suggestive of sustained animal-to-animal transmission and perhaps reflective of host adaptation. This suggests that continuous molecular surveillance of SARS-CoV-2 animal isolates is likely to reveal new insights into SARS-CoV-2 host range and adaptation, and may contribute to our understanding of risk for spillback of new variants. This also highlights the need to monitor for similar patterns of susceptibility to infection and sustained intra-species transmission in related

species. Our study draws attention to several specific, statistically significant nucleotide and amino acid substitutions that may play a role in host adaptation, pathogenesis, and/or transmission and are candidates for experimental study.

Methods

Data: On February 28, 2022, we downloaded from GISAID all SARS-CoV-2 consensus genome sequences derived from non-human animals. These host species include several mammalian species such as whitetail deer, mink, cats, dogs, lions, and monkeys among others. The raw non-human dataset obtained from GISAID was filtered for low-quality sequences, sequences with a length of less than 29k base pairs, and an ambiguous nucleotide (N) count above 500. Sequences with incomplete dates recorded in the metadata were discarded and excluded from the study. This study focuses on species with at least 30 sequences in the dataset, namely mink (n=1038), deer (n=134), cat (n=78), and dog (n=39).

From the 7.6 million human-derived viral sequences present in GISAID's human alignment dated February 28, 2022, a set of closely related sequences for every animal species was extracted. To do so, we used Nextstrain (Hadfield et al. 2018) to calculate a proximity matrix based on pairwise substitutions between every animal-derived sequence and all ~8 million human-derived sequences. The query alignment was generated using MAFFT (Katoh and Standley 2013) in which animal sequences were aligned to the gapped version of the Wuhan Iv04 reference sequence present in GISAID's human-host alignment dated February 28, 2022, with the "keeplength" option of the software enabled to maintain the length of context alignment in the query alignment.

Using this matrix and noting that some sequences from a given species might share a number of close relatives, we extracted the closest human-derived sequences for every sequence of a given species such that the unique set of best-hit human-host sequences for a particular species would have roughly the same count as the sequences from that animal species. To provide greater and more representative phylogenetic context, 500 human-derived sequences were subsampled randomly from every month of the pandemic, from January 2020 to February 2022, resulting in 13,000 human-derived sequences, distributed uniformly over time. Here again, the same quality filtering criteria were applied and the sample was drawn from sequences that were at least 29000

437 base pairs long and had fewer than 500 ambiguous nucleotides ("N" characters). The GISAID
438 identifiers for all sequences used in this study are reported in **Supplementary Table S1**.
439
440 **Alignment:** All the above sequences, that is, the animal-host sequences along with their closely
441 related human host sequences and the context random human subsample, and the Wuhan IV04
442 reference sequence were aligned using MAFFT (version 7.471). We used the NW-NS-2 setting,
443 which is a speed-oriented, progressive method without FFT approximation. The alignment was
444 done in two steps; first, a preliminary alignment was done and problematic sequences causing
445 almost invariant insertions due to stretches of ambiguous nucleotides (N's) were removed from
446 the dataset, and the remaining sequences were aligned again with the exact same algorithm,
447 resulting in the final alignment, including a total of 14787 sequences, comprised of 1038 mink
448 sequences, 134 deer sequences, 39 dog sequences, and 78 cat sequences. As for the closely
449 related human-host sequences, this dataset included 852 close relatives for mink, 61 for cat, 31
450 for dog, and 123 for deer. The remaining sequences were human-host sequences randomly
451 subsampled.
452
453 **Phylogeny:** Ten replicate trees for each candidate species were generated, each of which
454 included the focal species' sequences, its closely related human-host sequences, and one-tenth
455 of the randomly subsampled human-host sequences which were again split uniformly over time
456 to ensure temporal heterogeneity, resulting in an overall count of 40 trees. Maximum-likelihood
457 divergence trees were inferred using IQ-TREE (Nguyen et al. 2015) with a general time-reversible
458 model and with 1000 bootstrap iterations. The resulting trees were pruned for branches that are
459 unreasonably divergent, and tips whose lengths were considered outliers according to the
460 interquartile criterion and were longer than $q_{0.75} + 1.5IQR$ were pruned. $q_{0.75}$ in the above term
461 refers to the third quartile, and IQR refers to the difference between the first and the third quartiles.
462 This criterion discarded a maximum of 5 deer sequences out of 134, a maximum of 2 mink sequences
463 out of 1038, and a maximum of 1 dog sequence out of 39, while no cat sequences were pruned.
464
465 **Ancestral state reconstruction**: Discrete ancestral state reconstruction was performed on all 40
466 trees in the study, with states set as "human" and "animal". The reconstruction was done using
467 the maximum likelihood method "ace" implemented in the "ape" R package (Paradis and Schliep
468 2019). Ancestral state reconstruction was done using the "equal rates model" which allows for an
469 equal probability of transition in both directions of "animal to human" and "human to animal" on
470 the tree.

Estimating transmission events: Once the states were labeled, the set of all branches along which a transition from an “animal” node state to a “human” node state has occurred was identified, and the human end of the branch, namely the most recent common ancestor of the introduced human clade or the human tip in case of singletons, was marked as a transition node. In order to identify an independent set of transitions and to avoid the redundancy of reporting nested spilled-back clades as separate events, the most basal of these transition nodes were identified. In order to provide a well-rounded record of spillovers, the same analysis was done in the human to animal direction as well. For setting a lower bound to the transmission counts, in another set of analyses, all transitions in the desired direction were identified, then the branches whose parent side had a bootstrap support of lower than 75% were discarded, and subsequently, the most basal transitions were identified. To validate the ancestral state reconstruction and the transmission counts, a permutation test was done in which the tips of every 10 trees for all candidate species were randomly shuffled in 1000 permutations, and the same algorithm for ancestral state reconstruction and subsequently counting transitions in both directions (animal to human and human to animal) was applied to find the most basal transitions, unfiltered counts on the shuffled trees.

Genome-wide association studies: We used POUTINE (Chen and Shapiro 2021) to scan the genome for mutations that are statistically associated with each animal species. POUTINE relies on the viral phylogeny to identify homoplasic mutations associated with a phenotype of interest, in this case human vs. animal hosts. By considering only homoplasic mutations at the tips of the tree, POUTINE implicitly accounts for population structure. POUTINE was run on the 40 tree replicates (10 per species) and in each run, animal-host sequences were set as “cases” and human-host sequences as “controls.” We chose to treat animals as cases because the root of the tree is human, and initial transmission events are human-to-animal with more recent and rare animal-to-human events. The dataset is, therefore, better suited to identify animal-associated mutations than human-associated mutations. In each of the ten replicates for every species, any sites with a minor allele familywise p-value of less than 0.05 were recorded as a hit for that run. The unique collective set of hits for every species across all 10 runs was retained and the number of replicates in which each hit appeared was recorded.

Fisher’s exact test for geographic bias: In order to check for geographical bias we performed a Fisher’s exact test on every SNV identified by POUTINE to compare its frequency in human

hosts inside and outside regions where animal-host sequences bearing these mutations are found. For each SNV, we obtained its geographical distribution of human-host sequence counts broken down by geographical division from CoV-Spectrum. We partitioned global divisions into regions that animal-host sequences bearing the specific mutation are found in–namely, “in” regions, and regions in which such sequences are not found, or “out” regions. We then created the 2 by 2 contingency table in which rows correspond to wildtype allele and alternate (animal-associated) allele counts, and columns correspond to “in” or “out” region counts. We then calculated the pointwise estimate and confidence interval for the odds ratio, and flagged mutations in which the two frequencies were significantly different. Counts and frequencies for this step are recorded in Supplementary tables S4 and S5.

Code availability: Scripts used to perform all analyses are available at https://github.com/Saannah/Animal.SARS-CoV-2.git

Acknowledgments. We thank all the authors, developers, and contributors to the GISAID database for making their SARS-CoV-2 sequences publicly available. We are grateful to CoVaRR-Net colleagues Sally Otto, Art Poon, Caroline Colijn, Will Hsiao, Fiona Brinkman, Paul Gordon, Arinjay Banerjee, Jason Kindrachuk, Angie Rasmussen, and Samira Mubareka for useful discussions that helped improve the manuscript.

Funding. This study was supported by the Canadian Institutes for Health Research (CIHR) operating grant to the Coronavirus Variants Rapid Response Network (CoVaRR-Net). Data analyses were enabled by computing and storage resources provided by Compute Canada and Calcul Québec.

Supplementary Figures

Figure S1. Detailed representative phylogeny of cat- and human-derived SARS-CoV-2 sequences. In order to make the tree topology clear, branch lengths are not to scale.

Figure S2. Detailed representative phylogeny of dog- and human-derived SARS-CoV-2 sequences. In order to make the tree topology clear, branch lengths are not to scale.

Figure S3 Detailed representative phylogeny of mink- and human derived SARS-CoV-2 sequences. In order to make the tree topology clear, branch lengths are not to scale. The coloured boxes to the right of the tree show the allelic state of the three mink-associated GWAS hits in each terminal branch of the phylogeny.

Figure S4. Detailed representative phylogeny of deer- and human derived SARS-CoV-2 sequences. In order to make the tree topology clear, branch lengths are not to scale. The coloured boxes to the right of the tree show the allelic state of the seven deer-associated GWAS hits that appeared in all ten replicate GWAS runs.

Supplementary Tables

Table S1. GISAID accession numbers of all sequences used in this study.

Table S2. Number of viral sequences passing quality filters. The counts show the initial number of sequences downloaded from GISAID from each animal species, and the remaining number after each consecutive quality filter. The 'quality control' count shows the number of sequences after removing those with incomplete sampling dates and/or >500 ambiguous bases (Ns). The 'post-alignment pruning' shows the count after removing sequences shorter than 29,000 bases and/or with an insertion absent in all other sequences (introducing a gap in the alignment). The 'divergent tree branches' shows the count after removing sequences that introduce long branches into the phylogeny (Methods). Ranges of counts indicate variation across tree replicates.

Species	*Raw downloaded (N sequences)*	*Post-quality control*	*Post-alignment pruning*	*Post-divergent tree branch pruning*
mink	1339	1046	1038	1036
deer	156	153	134	129-133
cat	120	100	78	78
dog	76	59	39	38-39

Table S3. Table of transmission counts for all candidate species, in both animal to human and human to animal direction, for both bootstrap-filtered and unfiltered cases.

Species	Replicate	Animal to human (Bootstrap-filtered)	Animal to human (Un-filtered)	Human to animal (Bootstrap-filtered)	Human to animal (Un-filtered)
Mink	1	15	138	21	63
Mink	2	9	111	14	66
Mink	3	6	116	13	69
Mink	4	10	107	9	62
Mink	5	18	40	13	68
Mink	6	9	134	8	65
Mink	7	10	125	10	67
Mink	8	27	105	14	65
Mink	9	10	91	13	65
Mink	10	11	116	13	64
Deer	1	0	0	10	58
Deer	2	1	1	14	58
Deer	3	0	0	11	59
Deer	4	0	1	10	59
Deer	5	0	0	13	58
Deer	6	2	2	14	56
Deer	7	0	1	8	63
Deer	8	0	2	10	61
Deer	9	0	0	14	62
Deer	10	0	4	12	61
Cat	1	0	5	7	69
Cat	2	0	4	11	68
Cat	3	0	5	5	68
Cat	4	0	4	11	69
Cat	5	0	5	5	68

Cat	6	0	5	7	68
Cat	7	0	4	13	69
Cat	8	0	4	11	68
Cat	9	0	4	11	68
Cat	10	0	4	4	68
Dog	1	0	4	5	35
Dog	2	0	1	8	36
Dog	3	0	1	7	37
Dog	4	0	2	3	37
Dog	5	0	3	4	36
Dog	6	1	3	2	36
Dog	7	0	1	4	35
Dog	8	0	1	3	36
Dog	9	0	1	6	36
Dog	10	0	2	4	35

573 **Table S4.** Human-derived sequence counts bearing each of the significant GWAS hits identified
574 in deer inside and outside regions where deer sequences containing each mutation are
575 found. Odds ratio and the p-values are reported following a Fisher's exact test. GWAS hits
576 with OR < 1 or not significantly different from 1 are highlighted in green.

577

Position	Alternate allele count in deer regions	Wildtype allele count in deer regions	Alternate allele count outside deer regions	Wildtype allele count outside deer regions	Frequency of alternate allele in deer regions	Frequency of alternate allele outside deer regions	p_value	Conclusion
7303	433	838982	2226	10804361	0.000516101656531368	0.0002	8.6862e-56	ratio higher in deer regions
9430	1812	946458	9313	10688419	0.0019145065074203	0.0009	1.2416e-172	ratio higher in deer regions
14960	0	268814	266	11376922	0	2.3381e-05	0.0035	ratio lower in deer regions
20259	21	446625	417	11198939	4.70193115029387e-05	3.7236e-05	0.3171	ratio not significantly different
28016	20	213258	176	11432548	9.37831171632483e-05	1.5395e-05	8.6845e-10	ratio higher in deer regions
12073	210	321652	7184	11316956	0.000652879509532041	0.0006	0.6703	ratio not significantly different
29679	180	289240	2231	11354351	0.000622320564237312	0.0002	2.80664e-37	ratio higher in deer regions
5184	7012	238828	126835	11273327	0.0293600415361683	0.0112	0	ratio higher in deer regions
29750	1442	577400	8856	11058304	0.00249740214755802	0.0008	2.2500e-267	ratio higher in deer regions
7318	131	272041	1440	11372390	0.000481545061222389	0.0001	9.5330e-35	ratio higher in deer regions
16466	316970	860090	864781	9604161	0.368531200223232	0.0900	0	ratio higher in deer regions
7267	181	206553	3597	11435671	0.000876288410238534	0.0003	2.1368e-31	ratio higher in deer regions
210	307476	869584	854780	9614162	0.353589762461131	0.0889	0	ratio higher in deer regions

6730	32	20464	10034	11615472	0.00156372165754496	0.0007	0.0018	ratio higher in deer regions
27752	306844	870216	842927	9626015	0.35260670913888	0.0876	0	ratio higher in deer regions
11152	196	301370	9246	11335190	0.000650363340743936	0.0008	0.0013	ratio lower in deer regions
5822	7	39079	3456	11603460	0.00017912433787968	0.0003	0.2361	ratio not significantly different
9711	26	391615	1331	11253030	6.63917367822989e-05	0.0001	0.0020	ratio lower in deer regions
9679	79	561506	673	11083744	0.000140693064722372	6.0719	2.1058e-10	ratio higher in deer regions
7029	7	157363	2276	11486356	4.44831377134396e-05	0.0002	4.4009e-07	ratio lower in deer regions
29738	17	20479	11278	11614228	0.000830118658137604	0.0001	0.6520	ratio not significantly different
26767	318642	858418	871184	9597758	0.371196782919277	0.0908	0	ratio higher in deer regions
203	726	72179	19565	11553532	0.0100583272142867	0.0017	6.16135e-297	ratio higher in deer regions
12820	10	20486	1255	11624251	0.00048813824074978	0.0001	0.0001	ratio higher in deer regions
4540	322	195956	6718	11443006	0.00164322603033334	0.0006	7.7575e-55	ratio higher in deer regions
29666	1940	513027	27323	11103712	0.00378147738812967	0.0025	3.2392e-66	ratio higher in deer regions

584 **Table S5.** Human-derived sequence counts bearing each of the significant GWAS hits
585 identified in mink inside and outside regions where mink sequences containing each
586 mutation are found. Odds ratio and the p-values are reported following a Fisher's exact
587 test. GWAS hits with OR < 1 or not significantly different from 1 are highlighted in green.

588

Position	Alternate allele count in mink regions	Wildtype allele count in mink regions	Alternate allele count outside mink regions	Wildtype allele count outside mink regions	Frequency of alternate allele in mink regions	Frequency of alternate allele outside mink regions	p_value	Conclusion
26047	23	239184	279	11406516	9.6160e-05	2.44597035589132e-05	1.11877702252856e-07	ratio higher in mink regions
12795	34	152594	340	11493034	0.0002	2.95831370550196e-05	2.75263696173362e-18	ratio higher in mink regions
23064	67	296468	5363	11344104	0.0002	0.000472756596730777	1.43477105492256e-11	ratio lower in mink regions

589

590 **References**

591 Adney, Danielle R., Jamie Lovaglio, Jonathan E. Schulz, Claude Kwe Yinda, Victoria A.
592 Avanzato, Elaine Haddock, Julia R. Port, et al. 2022. "Severe Acute Respiratory Disease in
593 American Mink (Neovison Vison) Experimentally Infected with SARS-CoV-2." *bioRxiv*.
594 https://doi.org/10.1101/2022.01.20.477164.
595 Bosco-Lauth, Angela M., Airn E. Hartwig, Stephanie M. Porter, Paul W. Gordy, Mary Nehring,
596 Alex D. Byas, Sue VandeWoude, Izabela K. Ragan, Rachel M. Maison, and Richard A.
597 Bowen. 2020. "Experimental Infection of Domestic Dogs and Cats with SARS-CoV-2:
598 Pathogenesis, Transmission, and Response to Reexposure in Cats." *Proceedings of the*
599 *National Academy of Sciences of the United States of America* 117 (42): 26382–88.
600 Cai, Hugh Y., and Allison Cai. 2021. "SARS-CoV2 Spike Protein Gene Variants with N501T and
601 G142D Mutation-Dominated Infections in Mink in the United States." *Journal of Veterinary*
602 *Diagnostic Investigation: Official Publication of the American Association of Veterinary*
603 *Laboratory Diagnosticians, Inc* 33 (5): 939–42.
604 Cao, Zengguo, Hongjie Xia, Ricardo Rajsbaum, Xianzhu Xia, Hualei Wang, and Pei-Yong Shi.
605 2021. "Ubiquitination of SARS-CoV-2 ORF7a Promotes Antagonism of Interferon
606 Response." *Cellular & Molecular Immunology* 18 (3): 746–48.
607 Chen, Chaoran, Sarah Nadeau, Michael Yared, Philippe Voinov, Ning Xie, Cornelius Roemer,
608 and Tanja Stadler. 2021. "CoV-Spectrum: Analysis of Globally Shared SARS-CoV-2 Data
609 to Identify and Characterize New Variants." *Bioinformatics* , December.
610 https://doi.org/10.1093/bioinformatics/btab856.
611 Chen, Peter E., and B. Jesse Shapiro. 2021. "Classic Genome-Wide Association Methods Are
612 Unlikely to Identify Causal Variants in Strongly Clonal Microbial Populations." *bioRxiv*.
613 https://doi.org/10.1101/2021.06.30.450606.
614 De Maio, Nicola, Chieh-Hsi Wu, Kathleen M. O'Reilly, and Daniel Wilson. 2015. "New Routes to
615 Phylogeography: A Bayesian Structured Coalescent Approximation." *PLoS Genetics* 11 (8):
616 e1005421.
617 Di Giorgio, Salvatore, Filippo Martignano, Maria Gabriella Torcia, Giorgio Mattiuz, and Silvestro
618 G. Conticello. 2020. "Evidence for Host-Dependent RNA Editing in the Transcriptome of
619 SARS-CoV-2." *Science Advances* 6 (25): eabb5813.
620 Eckstrand, Chrissy D., Thomas J. Baldwin, Kerry A. Rood, Michael J. Clayton, Jason K. Lott,
621 Rebecca M. Wolking, Daniel S. Bradway, and Timothy Baszler. 2021. "An Outbreak of
622 SARS-CoV-2 with High Mortality in Mink (Neovison Vison) on Multiple Utah Farms." *PLoS*
623 *Pathogens* 17 (11): e1009952.
624 Elaswad, Ahmed, Mohamed Fawzy, Shereen Basiouni, and Awad A. Shehata. 2020.
625 "Mutational Spectra of SARS-CoV-2 Isolated from Animals." *PeerJ* 8 (December): e10609.
626 "Evolutionary Rate of SARS-CoV-2 Increases during Zoonotic Infection of Farmed Mink." 2022.
627 Virological. April 7, 2022. https://virological.org/t/evolutionary-rate-of-sars-cov-2-increases-
628 during-zoonotic-infection-of-farmed-mink/792.
629 Gilbert, Clément, and Torstein Tengs. 2021. "No Species-Level Losses of s2m Suggests Critical
630 Role in Replication of SARS-Related Coronaviruses." *Scientific Reports* 11 (1): 16145.
631 Hadfield, James, Colin Megill, Sidney M. Bell, John Huddleston, Barney Potter, Charlton
632 Callender, Pavel Sagulenko, Trevor Bedford, and Richard A. Neher. 2018. "Nextstrain:
633 Real-Time Tracking of Pathogen Evolution." *Bioinformatics* 34 (23): 4121–23.
634 Harris, Reuben S., and Jaquelin P. Dudley. 2015. "APOBECs and Virus Restriction." *Virology*
635 479-480 (May): 131–45.
636 Hillen, Hauke S., Goran Kokic, Lucas Farnung, Christian Dienemann, Dimitry Tegunov, and
637 Patrick Cramer. 2020. "Structure of Replicating SARS-CoV-2 Polymerase." *Nature* 584
638 (7819): 154–56.
639 Katoh, Kazutaka, and Daron M. Standley. 2013. "MAFFT Multiple Sequence Alignment

Software Version 7: Improvements in Performance and Usability." *Molecular Biology and Evolution* 30 (4): 772–80.

Kotwa, Jonathon D., Ariane Massé, Marianne Gagnier, Patryk Aftanas, Juliette Blais-Savoie, Jeff Bowman, Tore Buchanan, et al. 2022. "First Detection of SARS-CoV-2 Infection in Canadian Wildlife Identified in Free-Ranging White-Tailed Deer (Odocoileus Virginianus) from Southern Québec, Canada." *bioRxiv*. https://doi.org/10.1101/2022.01.20.476458.

Kuchipudi, Suresh V., Meera Surendran-Nair, Rachel M. Ruden, Michele Yon, Ruth H. Nissly, Kurt J. Vandegrift, Rahul K. Nelli, et al. 2022. "Multiple Spillovers from Humans and Onward Transmission of SARS-CoV-2 in White-Tailed Deer." *Proceedings of the National Academy of Sciences of the United States of America* 119 (6). https://doi.org/10.1073/pnas.2121644119.

Liu, Guanqun, Jung-Hyun Lee, Zachary M. Parker, Dhiraj Acharya, Jessica J. Chiang, Michiel van Gent, William Riedl, et al. 2021. "ISG15-Dependent Activation of the Sensor MDA5 Is Antagonized by the SARS-CoV-2 Papain-like Protease to Evade Host Innate Immunity." *Nature Microbiology* 6 (4): 467–78.

Liu, Yang, Jianying Liu, Kenneth S. Plante, Jessica A. Plante, Xuping Xie, Xianwen Zhang, Zhiqiang Ku, et al. 2021. "The N501Y Spike Substitution Enhances SARS-CoV-2 Infection and Transmission." *Nature*, November. https://doi.org/10.1038/s41586-021-04245-0.

Lu, Lu, Reina S. Sikkema, Francisca C. Velkers, David F. Nieuwenhuijse, Egil A. J. Fischer, Paola A. Meijer, Noortje Bouwmeester-Vincken, et al. 2021. "Adaptation, Spread and Transmission of SARS-CoV-2 in Farmed Minks and Associated Humans in the Netherlands." *Nature Communications* 12 (1): 6802.

Miao, Zhichao, Antonin Tidu, Gilbert Eriani, and Franck Martin. 2021. "Secondary Structure of the SARS-CoV-2 5'-UTR." *RNA Biology* 18 (4): 447–56.

Morales Lucia, Mateos-Gomez Pedro A., Capiscol Carmen, del Palacio Lorena, Enjuanes Luis, and Sola Isabel. 2013. "Transmissible Gastroenteritis Coronavirus Genome Packaging Signal Is Located at the 5′ End of the Genome and Promotes Viral RNA Incorporation into Virions in a Replication-Independent Process." *Journal of Virology* 87 (21): 11579–90.

Murall, Carmen Lía, Eric Fournier, Jose Hector Galvez, Arnaud N'Guessan, Sarah J. Reiling, Pierre-Olivier Quirion, Sana Naderi, et al. 2021. "A Small Number of Early Introductions Seeded Widespread Transmission of SARS-CoV-2 in Québec, Canada." *Genome Medicine* 13 (1): 169.

Newman, Joseph A., Alice Douangamath, Setayesh Yadzani, Yuliana Yosaatmadja, Antony Aimon, José Brandão-Neto, Louise Dunnett, et al. 2021. "Structure, Mechanism and Crystallographic Fragment Screening of the SARS-CoV-2 NSP13 Helicase." *Nature Communications* 12 (1): 4848.

Nguyen, Lam-Tung, Heiko A. Schmidt, Arndt von Haeseler, and Bui Quang Minh. 2015. "IQ-TREE: A Fast and Effective Stochastic Algorithm for Estimating Maximum-Likelihood Phylogenies." *Molecular Biology and Evolution* 32 (1): 268–74.

Oreshkova, Nadia, Robert Jan Molenaar, Sandra Vreman, Frank Harders, Bas B. Oude Munnink, Renate W. Hakze-van der Honing, Nora Gerhards, et al. 2020. "SARS-CoV-2 Infection in Farmed Minks, the Netherlands, April and May 2020." *Euro Surveillance: Bulletin Europeen Sur Les Maladies Transmissibles = European Communicable Disease Bulletin* 25 (23). https://doi.org/10.2807/1560-7917.ES.2020.25.23.2001005.

Otto, Sarah P., Troy Day, Julien Arino, Caroline Colijn, Jonathan Dushoff, Michael Li, Samir Mechai, et al. 2021. "The Origins and Potential Future of SARS-CoV-2 Variants of Concern in the Evolving COVID-19 Pandemic." *Current Biology: CB* 0 (0). https://doi.org/10.1016/j.cub.2021.06.049.

Oude Munnink, Bas B., Reina S. Sikkema, David F. Nieuwenhuijse, Robert Jan Molenaar, Emmanuelle Munger, Richard Molenkamp, Arco van der Spek, et al. 2021. "Transmission of SARS-CoV-2 on Mink Farms between Humans and Mink and back to Humans." *Science*

371 (6525): 172–77.
Paradis, Emmanuel, and Klaus Schliep. 2019. “Ape 5.0: An Environment for Modern Phylogenetics and Evolutionary Analyses in R.” *Bioinformatics* 35 (3): 526–28.
Pickering, Bradley, Oliver Lung, Finlay Maguire, Peter Kruczkiewicz, Jonathan D. Kotwa, Tore Buchanan, Marianne Gagnier, et al. 2022. “Highly Divergent White-Tailed Deer SARS-CoV-2 with Potential Deer-to-Human Transmission.” *bioRxiv*. https://doi.org/10.1101/2022.02.22.481551.
Redondo, Natalia, Sara Zaldívar-López, Juan J. Garrido, and Maria Montoya. 2021. “SARS-CoV-2 Accessory Proteins in Viral Pathogenesis: Knowns and Unknowns.” *Frontiers in Immunology* 12 (July): 708264.
Rosenberg, Brad R., Claire E. Hamilton, Michael M. Mwangi, Scott Dewell, and F. Nina Papavasiliou. 2011. “Transcriptome-Wide Sequencing Reveals Numerous APOBEC1 mRNA-Editing Targets in Transcript 3’ UTRs.” *Nature Structural & Molecular Biology* 18 (2): 230–36.
Salter, Jason D., and Harold C. Smith. 2018. “Modeling the Embrace of a Mutator: APOBEC Selection of Nucleic Acid Ligands.” *Trends in Biochemical Sciences* 43 (8): 606–22.
Sheahan, Timothy P., Amy C. Sims, Shuntai Zhou, Rachel L. Graham, Andrea J. Pruijssers, Maria L. Agostini, Sarah R. Leist, et al. 2020. “An Orally Bioavailable Broad-Spectrum Antiviral Inhibits SARS-CoV-2 in Human Airway Epithelial Cell Cultures and Multiple Coronaviruses in Mice.” *Science Translational Medicine* 12 (541). https://doi.org/10.1126/scitranslmed.abb5883.
Shi, Jianzhong, Zhiyuan Wen, Gongxun Zhong, Huanliang Yang, Chong Wang, Baoying Huang, Renqiang Liu, et al. 2020. “Susceptibility of Ferrets, Cats, Dogs, and Other Domesticated Animals to SARS-Coronavirus 2.” *Science* 368 (6494): 1016–20.
Shin, Donghyuk, Rukmini Mukherjee, Diana Grewe, Denisa Bojkova, Kheewoong Baek, Anshu Bhattacharya, Laura Schulz, et al. 2020. “Papain-like Protease Regulates SARS-CoV-2 Viral Spread and Innate Immunity.” *Nature* 587 (7835): 657–62.
Starr, Tyler N., Allison J. Greaney, Sarah K. Hilton, Daniel Ellis, Katharine H. D. Crawford, Adam S. Dingens, Mary Jane Navarro, et al. 2020. “Deep Mutational Scanning of SARS-CoV-2 Receptor Binding Domain Reveals Constraints on Folding and ACE2 Binding.” *Cell* 182 (5): 1295–1310.e20.
Tan, Cedric C. S., Su Datt Lam, Damien Richard, Christopher J. Owen, Dorothea Berchtold, Christine Orengo, Meera Surendran Nair, et al. 2022. “Transmission of SARS-CoV-2 from Humans to Animals and Potential Host Adaptation.” *Nature Communications* 13 (1): 1–13.
Tengs, Torstein, Anja Bråthen Kristoffersen, Tsvetan R. Bachvaroff, and Christine Monceyron Jonassen. 2013. “A Mobile Genetic Element with Unknown Function Found in Distantly Related Viruses.” *Virology Journal* 10 (April): 132.
Vöhringer, Harald S., Theo Sanderson, Matthew Sinnott, Nicola De Maio, Thuy Nguyen, Richard Goater, Frank Schwach, et al. 2021. “Genomic Reconstruction of the SARS-CoV-2 Epidemic in England.” *Nature*, October. https://doi.org/10.1038/s41586-021-04069-y.
Wacker, Anna, Julia E. Weigand, Sabine R. Akabayov, Nadide Altincekic, Jasleen Kaur Bains, Elnaz Banijamali, Oliver Binas, et al. 2020. “Secondary Structure Determination of Conserved SARS-CoV-2 RNA Elements by NMR Spectroscopy.” *Nucleic Acids Research* 48 (22): 12415–35.
Wei, Changshuo, Ke-Jia Shan, Weiguang Wang, Shuya Zhang, Qing Huan, and Wenfeng Qian. 2021. “Evidence for a Mouse Origin of the SARS-CoV-2 Omicron Variant.” *bioRxiv*. https://doi.org/10.1101/2021.12.14.472632.
Worobey, Michael, Joshua I. Levy, Lorena M. Malpica Serrano, Alexander Crits-Christoph, Jonathan E. Pekar, Stephen A. Goldstein, Angela L. Rasmussen, et al. 2022. *The Huanan Market Was the Epicenter of SARS-CoV-2 Emergence*. https://doi.org/10.5281/zenodo.6299116.

742 Yang, Dong, and Julian L. Leibowitz. 2015. “The Structure and Functions of Coronavirus
743 Genomic 3’ and 5' Ends.” *Virus Research* 206 (August): 120–33.
744 Yen, Hui-Ling, Thomas H. C. Sit, Christopher J. Brackman, Shirley S. Y. Chuk, Haogao Gu,
745 Karina W. S. Tam, Pierra Y. T. Law, et al. 2022. “Transmission of SARS-CoV-2 Delta
746 Variant (AY.127) from Pet Hamsters to Humans, Leading to Onward Human-to-Human
747 Transmission: A Case Study.” *The Lancet* 399 (10329): 1070–78.
748 Zhou, Jie, Thomas P. Peacock, Jonathan C. Brown, Daniel H. Goldhill, Ahmed M. E. Elrefaey,
749 Rebekah Penrice-Randal, Vanessa M. Cowton, et al. 2022. “Mutations That Adapt SARS-
750 CoV-2 to Mink or Ferret Do Not Increase Fitness in the Human Airway.” *Cell Reports* 38 (6):
751 110344.

752